Cyclic out-of-plane behaviour of slender clay brick masonry walls seismically strengthened using posttensioning

Najif Ismail, S.M. ASCE
PhD Student, Department of Civil & Environmental Engineering, University of Auckland, Private Bag 92019, Auckland 1142, New Zealand; nism009@aucklanduni.ac.nz

Jason M. Ingham, M. ASCE
Associate Professor, Department of Civil & Environmental Engineering, University of Auckland, Private Bag 92019, Auckland 1142, New Zealand; j.ingham@auckland.ac.nz

Abstract

Equations for the design of a posttensioned seismic retrofit of unreinforced clay brick masonry walls are discussed and results from an associated experimental program are reported. A total of eight (08) full scale multi-wythe vintage solid clay brick masonry walls were subjected to uniformly distributed one directional and reverse cyclic out-of-plane loading, of which two (02) walls were tested as-built and six (06) walls were seismically retrofitted using unbonded posttensioning. Test wall configurations and constituent masonry materials were selected to replicate typical characteristics of historic clay brick masonry walls. The test walls were seismically retrofitted by applying varying magnitudes of posttensioning using a single tendon, inserted into a cavity located at the centre of each test wall. Several aspects pertaining to the seismic behaviour of posttensioned masonry walls were investigated, including damage patterns, force-displacement behaviour, tendon stress variation, wall secant stiffness, hysteretic energy dissipation, toughness modulus, and damping ratio. Finally, measured performance parameters of the test walls were compared to the corresponding values predicted using the proposed design equations.

Keywords: cyclic; out-of-plane; masonry; seismic strengthening; posttensioning.

Introduction

It is well established that unreinforced masonry (URM) bearing wall buildings are prone to damage in moderate to large magnitude earthquakes, with their poor seismic performance routinely documented in various earthquake reconnaissance reports. The principal damaging failure mode to URM buildings observed in past earthquakes is out-of-plane failure of slender URM walls, which can result due to flexural failure of the wall and/or wall anchorage failure. The poor performance of URM buildings during the recent series of 2010/2011 New Zealand earthquakes was consistent with that anticipated after a large magnitude earthquake, with the majority of URM buildings located in Christchurch observed to have partially or completely collapsed (Dizhur et al. 2010, Ingham and Griffith 2011, Ingham et al. 2011). The two options available to alleviate the risk of collapse of URM buildings in a large earthquake are either demolition or the implementation of a seismic retrofit, with the latter option being preferred in many instances due to concerns regarding the preservation of architectural heritage. One such retrofit technique is to apply vertical unbonded posttensioning to seismically deficient masonry walls.

As unbonded posttensioning is reversible to some extent and has minimal impact on the architectural fabric of the building, this type of retrofit intervention is deemed to be desirable for buildings having important heritage value. Another advantage of unbonded posttensioning is its proven track record in new posttensioned concrete and concrete masonry construction. In existing URM walls the added posttensioning is applied either by placing posttensioning (PT) tendons inside cored cavities located at the centre of the wall or by placing PT tendons externally at discrete locations. The first application procedure involves coring a cavity from the top of the URM wall right through to the foundation and then placing a tendon into the cored cavity, which is then posttensioned. One example of implementation of this technique is the Rob Roy tavern located in Auckland, New Zealand,

which was relocated from its original position and prior to the relocation was strengthened using shotcreting and unbonded posttensioning to withstand lateral forces generated due to movement of the building (NZTA 2010). Fig. 1(a) shows a photograph of the coring operation for inserting the PT tendons, which were dead-end anchored into the reinforced concrete beam at the wall base and then posttensioned and live-end anchored using specially cast concrete anchor blocks located at the top of the parapet. Alternatively, discretely located external unbonded posttensioning has also been used in retrofit projects, avoiding the coring operation. When using external posttensioning, PT tendons are typically located at re-entrant wall corners or in the recess of buttressed URM walls, or inside a URM cavity wall. One example of externally applied posttensioning is the Christchurch Arts Centre, as shown in Fig. 1(b).

History and Codification

Use of posttensioned in masonry buildings dates back to the 1950's, and was at first used to resist lateral wind loads and for structural components having unusual dimensions. Such applications involved prestressed fin walls, retaining walls, and storage tanks (Curtin et al. 1984). With subsequent developments, posttensioning was used to improve the seismic performance of URM walls, with several case studies of such applications reported by Ganz (1996). Further details on the development and history of prestressed masonry are reported by Schultz and Scolforo (1991).

The research and codification of posttensioned masonry originated from Switzerland and the United Kingdom and led to the inclusion in BS 5628-85 (1985) of provisions relating to prestressed masonry walls, which was updated in 1995 to include the design of concrete masonry (BS 1995) and was further revised in 2000 (BS 2000). The European Code first included prestressed masonry provisions in EC 6-95 (1995), which were later updated with the issue of EC 6-05 (2005). The Australian masonry code AS 3700-98 (1998) included

prestressed masonry for the first time, which was later revised in 2001 (AS 2001). In the United States, a draft amendment on prestressed masonry was completed in the 1990's (Scolforo 1996) and was then included in TMS 402-02 (MSJC 2002), which was updated in 2005 (MSJC 2005) and again in 2008 (MSJC 2008). Prestressed masonry design criteria were first included in the Canadian masonry code with the issue of CSA S304.1-04 (2004). The New Zealand masonry design standard NZS 4230-90 (1990) referred to the design of prestressed concrete masonry, being conceptually similar to the design of prestressed concrete. Later New Zealand research conducted on prestressed concrete masonry (Laursen 2002; Wight 2006) led to the inclusion of an ultimate strength design criteria for prestressed concrete masonry in the New Zealand Reinforced Concrete Masonry Design Standard NZS 4230-04 (2004). Unbonded posttensioning has also been referred to as a viable seismic retrofit solution in FEMA 547-06 (2006) and in ASCE/SEI 41-06 (2006), but a retrofit design criteria is not discussed directly. The research reported here was undertaken to investigate the development of predictive equations for posttensioning seismic retrofit design of URM buildings (Ismail 2011).

Past Testing

Previously performed experimental studies have investigated the out-of-plane behaviour of posttensioned masonry walls but were mainly focused on new construction, with no or minimal experimental results existing in the literature reporting the performance of seismically retrofitted historic URM walls subjected to out-of-plane loading. Brief details and key outcomes of some previously performed relevant experimental studies are discussed below.

One of the earliest research studies that investigated the performance of posttensioned masonry walls was conducted by Al-Manaseer and Neis (1987), involving out-of-plane testing of six (06) full scale concrete masonry walls. Of these six walls, two walls were

conventionally reinforced with mild steel reinforcing bars and the remaining four walls were posttensioned using various configurations of 12.7 mm high strength steel strands, with the PT strands stressed to 80% of their ultimate strength and placed inside grouted conduits. In all posttensioned wall tests, a single mortar joint at or near mid-height was observed to open on the wall tension face, being the typical out-of-plane failure mode also observed in other research studies. Force-displacement curves for the posttensioned walls revealed that the flexural capacity of the walls increased by up to 221% when compared to the strength of the two conventionally reinforced test walls having no prestress.

Krause et al. (1996) suggested that posttensioned concrete masonry walls perform similarly to prestressed concrete walls when subjected to lateral loading. Their experimental program consisted of out-of-plane testing of masonry walls constructed using two-cored clay brick units aligned to allow for a continuous cavity for PT tendons, with these walls designed using code provisions of the time (MSJC 1995). All test walls were posttensioned using high strength (f_{py} = 1000 MPa) 16 mm threaded steel bars, with an initial posttensioning force of 84.5 kN. All test walls exhibited a bilinear elastic behaviour and from test results it was established that posttensioning can be applied to clay brick masonry walls having a compressive strength similar to that of historic clay brick masonry.

The performance of posttensioned clay brick masonry walls has more recently been investigated in a series of experiments documented by Bean Popehn et al. (2007). A total of twelve (12) half scale simply supported URM walls, each being 3540 mm high × 800 mm long × 100 mm thick, were subjected to face loading. Of these test walls six (06) were built using clay brick masonry, with three (03) test walls posttensioned using unbonded tendons and three (03) test walls posttensioned using bonded tendons. Threaded steel bars were attached to the walls at their outermost edges and the seismic performance of posttensioned masonry walls having a large h/t ratio (38.0-40.5) was investigated by performing pseudo-

static structural testing. The walls exhibited linear elastic response up to the point of cracking and drifts of approximately 6% to 10% were achieved without wall collapse. Tendon stresses increased upon application of lateral loading, attributed to tendon elongation, with lateral shifting of unrestrained tendons observed during testing. Strength loss at large displacement was also observed, which was attributed to localised crushing of mortar at crack location.

Analysis and Design

The failure mode of out-of-plane loaded URM walls, having sufficient diaphragm anchorage, is characterised by the formation of one or several large horizontal cracks at or near wall mid-height, which form when the flexural tensile strength of the wall is exceeded and the wall begins to rock about the mid-height crack. When cracking initiates at wall mid-height, stress at the tension face of the wall reaches zero and on the compression face reaches a stress of twice the initial applied prestress. It should be noted that the first cracking limit state corresponds to the elastic limit of the wall and the moment capacity to cause cracking, M_c, can be evaluated by considering the equilibrium of forces (refer Equation 1).

$$M_c = \frac{l_w b_w^2}{6}(f_m + f_r) \text{ where: } f_m = \frac{N_t + 0.5W_w + f_{se}A_{ps}}{b_w l_w} \quad (1)$$

where: l_w = wall length; b_w = wall thickness; W_w = wall self-weight; N_t = over burden weight; f_{se} = effective tendon stress; f_r = masonry modulus of rupture and A_{ps} = cross sectional area of posttensioning tendon. The effective tendon stress, f_{se}, is determined by subtracting PT losses from the initially applied tendon stress, f_{psi}. It should be noted that accurate estimation of PT losses is crucial for the longevity of a retrofit design. Current masonry codes (AS 2001; CSA 2004; NEC 2005; NZS 2004; SMJC 2008) provide guidelines for assessing PT losses, with these losses typically attributed to shrinkage, creep, tendon relaxation, elastic shortening, anchorage seating, tendon undulation, friction and thermal effects. Of these factors, steel relaxation, shrinkage and creep are the most important factors

that will influence the design and longevity of an adequate retrofit. However, for historic clay brick masonry walls shrinkage losses or masonry expansion is unlikely to be significant because of the significant age of the masonry materials.

Predicting the seismic response of a posttensioned masonry wall at the nominal strength limit state requires accurate estimation of the maximum useable masonry strain at the extreme compression fibre, ε_{mu}, and increased tendon stress, f_{ps}, due to tendon elongation and corresponding tendon strain, ε_s. Fig. 2(a) shows a posttensioned URM wall that is subjected to transverse loading and Fig. 2(b) shows the resulting deformations at the nominal strength limit state, where the PT tendon has a modulus of elasticity, E_{ps}, and an effective tendon stress, f_{se}. The tendon stress at the nominal strength increases due to tendon elongation and can be presented as Equation 2, where ε_s is the tendon strain at nominal strength.

$$f_{ps} = f_{se} + E_{ps}\varepsilon_s \leq \min(0.85\, f_{py}, 0.7 f_{pu}) \quad (2)$$

At nominal strength the compression stress distribution at the compression face of the wall becomes non-uniform, which is typically approximated by an equivalent rectangular compression stress block (refer Fig. 3(b)). Table 1 presents codified values of the stress block parameters recommended for clay brick masonry. In the current study the parameters specified in NZS 4230-04 (2004) were adopted. Due to the higher deformability of prevalent weak lime mortar used in historic URM construction, the strain values predicted to occur at nominal strength were higher than that typically defined for URM i.e., 0.0035 (MSJC 2008). Therefore, the nominal strength for out-of-plane loaded posttensioned masonry walls is defined herein as the point when the out-of-plane drift, 2θ, reaches 3% and the corresponding masonry strain value is termed the maximum useable masonry strain (refer Fig. 3(a)). The nominal out-of-plane flexural strength of a posttensioned URM wall, M_n, is calculated in accordance with Equation 3 based on beam theory.

$$M_n = (N_t + 0.5W_w + f_{ps}A_{ps})\left[d - \frac{a}{2}\right] \quad (3)$$

$$\text{where: } a = \frac{(N_t + 0.5W_w + f_{ps}A_{ps})}{\alpha f'_m l_w} \text{ and } \alpha = 0.85$$

Where f'_m is the masonry compression strength and d is the minimum distance between the PT tendon centroid and the extreme compression fibre, typically being $\frac{b_w}{2}$ for a wall having rectangular plan geometry. The maximum tendon stress is taken as the smaller of $0.85f_{py}$ or $0.7f_{pu}$, where $0.7f_{pu}$ is generally the governing limitation, and is adopted in Equation 5. If the unbonded length of PT tendon is equal to the height of the wall, the rotation value is small, and both axial shortening due to elevated prestress and masonry deformation at the point of rotation are neglected then ε_s can be estimated using Equation 4, which was rewritten as Equation 5 by stipulating a maximum base rotation, θ, of 0.015. By substituting Equation 5 and values for constants α and β of 0.85 for both (typical in flexural design) into Equation 2, Equation 6 is obtained.

$$\varepsilon_s = \frac{2\theta}{h_e}(d - c) \quad (4)$$

$$\varepsilon_s = \frac{0.03d}{h_e}\left(1 - \frac{0.7f_{pu}A_{ps}}{\alpha\beta f'_m l_w d}\right) \quad (5)$$

$$f_{ps} = f_{se} + 0.03E_{ps}\left(\frac{d}{h_e}\right)\left[1 - 0.97\frac{f_{pu}A_{ps}}{f'_m l_w d}\right] \leq \min(0.85\, f_{py}, 0.7f_{pu}) \quad (6)$$

An equation similar to Equation 6 has been recommended and investigated by Bean Popehn and Schultz (2010) in a recent study using a data set from 127 finite element analyses and 66 test results, and was found to predict tendon stress better than current design expressions. However, it should be noted that Equation 6 is based on tendon elongation due to a single mid-height crack opening, whereas in walls having more than one hinge locations (e.g., opening of several mid-height cracks in multi-storey walls) tendon elongation depends upon the number of hinge locations (refer Fig. 4). Therefore, Equation 7 can be used to ensure that the elevated tendon stress for a multi-storey wall effectively secured at all

diaphragm levels and having n number of storeys remains within elastic limits when in a worst case scenario cracks opens at each storey level. It should be noted that the wall may or may not crack at each storey level and that the tendon stress predicted using Equation 7 in the latter case will result in over predicted nominal strength of the wall.

$$f_{ps} = f_{se} + 0.06E_{ps}\sum_{i=1}^{n}\left(\frac{d_i}{h_{ei}}\right)\left[1 - 0.97\frac{f_{pu}A_{ps}}{f'_m l_{wi} d_i}\right] \leq \min(0.85\, f_{py},\ 0.7f_{pu}) \quad (7)$$

where d_i is the minimum distance of tendon centroid from extreme the compression fibre on either side of the wall for the ith storey and h_{ei} is the effective height of the wall for the ith floor.

Experimental Program

An experimental program was undertaken to investigate the structural performance of clay brick masonry walls retrofitted using posttensioning, which involved material testing of constructed masonry assemblages and full scale out-of-plane testing of posttensioned slender clay brick masonry walls. The full scale out-of-plane testing program consisted of two series of tests (series 1 and series 2). Series 1 testing involved one directional cyclic out-of-plane testing of three (03) full scale slender masonry walls, each being 4.1 m high × 1.2 m long and 220 mm (two-wythe) thick. Series 2 testing involved two directional (reverse) cyclic out-of-plane testing of five (05) full scale slender masonry walls, each being 3.67 m high × 1.2 m long and 220 mm (two-wythe) thick. The selected wall configurations were representative of common seismically deficient out-of-plane loaded clay brick unreinforced masonry walls, achieving a low percentage of new building strength when evaluated using the New Zealand Society for Earthquake Engineering guidelines (NZSEE 2006). Two (02) walls (one from each testing series) were tested as-built to serve as control walls, and six (06) walls were seismically strengthened prior to testing using different levels of posttensioning. Test walls were given the notation ABO-N or PTO-N, where AB refers to as-built tested walls, PT

refers to posttensioned walls, O refers to out-of-plane testing and N denotes the test number. Test wall dimensions and posttensioning details are shown in Table-2.

Material Properties

All test walls were constructed using a common bond pattern, with one header course located after every three stretcher courses using roughly 15 mm thick mortar courses. The bond pattern was selected because of its prevalence in existing historic URM construction. Salvaged solid clay bricks, being 220 mm long × 105 mm wide × 75 mm high, and a hydraulic cement mortar with a mix ratio of 1:2:9 (cement:lime:sand) was used, replicating historic URM construction.

Masonry modulus of rupture was determined by testing 24 three brick high masonry prisms for flexural strength in accordance with AS/NZS 4456.15 (2003), typically 2 for each test wall. Mortar compressive strength was determined by testing twenty 50 mm mortar cubes in accordance with ASTM C109/C109M (2002) and the compressive strength of bricks and masonry were determined in accordance with ASTM C270 (2003) and ASTM C62 (2004) respectively, typically in sets of two for each test wall. Masonry cohesion, C, and coefficient of friction, μ, were investigated by bed joint shear testing of 6 three brick high prisms that were subjected to varying magnitudes of axial compression stress applied using externally posttensioned bars. The results of material testing are reported in Table 3 as mean values and corresponding coefficients of variation (COV).

Two different types of PT tendons were used for posttensioning the test walls, being threaded mild steel bar (with tensile yield strength of 500 MPa) and sheathed greased seven wire strands (with tensile yield strength of 1680 MPa). Threaded steel bars are typically used for straight posttensioning over short distances. The greased coating of strands enables high corrosion resistance and lower frictional losses, which makes them an ideal choice for unbonded and/or external posttensioning applications.

Posttensioning Details

As maximum masonry compression stresses develop at mid-height (hinge zone) when the slender vertically spanning masonry walls were subjected to out-of-plane seismic excitations, a single PT tendon with bearing plates was adequate to produce the required stresses in the hinge zone by distributing axial compression stress at an angle of 45^{o} from the end anchorage and into the wall. Therefore, all test walls were posttensioned using one PT tendon (threaded bar or strand) inserted inside a formed circular cavity at the centre of the wall, and steel bearing plates were used to avoid localized masonry crushing. A flexible circular conduit (roughly 25 mm diameter) was inserted during construction to provide the circular cavity in the test walls, and bricks were accordingly chiselled to accommodate the conduit. As there was no bond between masonry and tendon, the conduit encased tendon behaved as if it was placed in a cored circular cavity.

To transfer prestress to the test walls, end anchorages (flat base hexagonal nuts for threaded bar and standard steel barrel anchors with wedges for the strand) were locked off onto steel plates (each being 220 mm × 220 mm × 50 mm) at the top and bottom of the wall, which performed adequately and the masonry around the steel bearing plates sustained the compression stresses without any signs of cracking. In order to make the strand posttensioning reversible (i.e., to remove the strand) a 40 mm thick mild steel plate split in two halves was used, which was removable to destress the strand once testing was concluded. Threaded mild steel bars were posttensioned using a 100 kN hydraulic jack, which was removed after tightening of the nut that clasped the PT bar. For posttensioning of the seven wire greased strand an electronically operated hydraulic jack was used, and the taut strand was clasped by wedge interlocking.

Testing Details

Series 1 testing was performed using the air bag rig shown in Fig. 5(a), consisting of a

backing frame, a rigid steel reaction frame anchored to the concrete floor, two air bags capable of withstanding 15 kPa air pressure, four S shape 10 kN load cells, two pairs of frictionless plates, and a linear variable differential transducer with stand (Derakhshan 2011). For series 2 testing, four air bags were used to apply a uniformly distributed reverse cyclic pseudo-static loading, emulating a lateral seismic load generated in the out-of-plane direction. A backing frame was located on each side of the wall, being supported by four equally spaced 10 kN S-shape load cells sandwiched between the backing frame and the strong reaction frame. The test setup used to perform series 2 testing is shown in Fig. 5(b).

In both testing series, one linear variable differential transducer was located at wall mid-height to determine lateral displacement. When air bags were inflated using the air compressor, the backing frame exerted force to S-shape load cells measuring the applied load on the test wall. Each backing frame was placed over two pairs of smooth greased steel plates having negligible friction, such that the backing frame self-weight did not impair the test results. The rigid reaction frame acted as a backing and also supported the top of the wall, creating boundary conditions comparable to those when a posttensioned wall is connected to a floor or ceiling diaphragm. For all posttensioned walls a 200 kN load cell was located between the tendon anchorage and the top of the wall, to record the force in the PT tendon. A displacement controlled loading history was applied by inflating and deflating the air bags alternatively. Each cycle was repeated twice and displacement was increased gradually as a function of drift values up to a maximum of 4%.

Experimental Results and Discussion

Table 4 gives an overview of the test results. First cracking moment, tendon stress at nominal strength, and nominal flexural capacity for each test wall were predicted using Equations 1, 3 and 6. The predicted values were then compared to measured experimental

values and the validity of the proposed design equations was checked. To quantify the ductility of test walls a maximum measured drift ratio was defined as $\gamma_u = \frac{2\Delta_u}{h_e}$, where Δ_u is the maximum measured mid-height displacement and h_e is the effective height of the wall. Test wall PTO-03 was loaded until its post peak strength degraded to nearly half of the measured flexural strength, and test walls PTO-04 to PTO-07 did not reach their flexural capacity before testing was terminated due to safety concerns. Therefore, it should be noted that the maximum measured drift values reported in Table 4 for walls PTO-4 to PTO-07 are not representative of the ultimate achievable drift values. In a previous experimental study reported by Ismail et al. (2011), a maximum drift of up to 11.9% was observed for posttensioned masonry walls.

Crack Patterns

Figs. 6 (a to c) show photographs of the test setup and deflected test walls. A single large crack at or near mid-height was observed in all tests except PTO-08 that failed prematurely in shear at a location above the airbag, which was attributed to a low modulus of rupture and is not likely to happen when walls are subjected to a uniformly distributed lateral load over the entire wall height. A rocking failure mode without any distributed flexural cracking was observed during the testing, with damage concentrated at one bed joint location and the wall returning to its original position upon unloading. The observed damage pattern would require minor post-earthquake repairs, which is deemed advantageous for enabling immediate occupancy following an earthquake. In test wall PTO-03 the threaded mild steel bar reached its elastic limit and possibly yielded (causing strength degradation) but no visible residual deflections were observed.

Force-Displacement Response

Figs. 7 (a to f) show the measured force-displacement response for each of the test

walls, with a dotted line showing the predicted nominal flexural strength of the wall. All force-displacement histories were plotted with analogous moment and drift values on a secondary axis to allow comparison between the results of test walls having different heights. The results of the corresponding as-built tested wall are also plotted (dotted line), to illustrate the seismic improvement due to posttensioning. Self-centering behaviour was observed during testing, with walls returning to their original position upon unloading. Test walls PTO-04 to PTO-07 did not reach their maximum strength, which would result from either tendon yielding or after reaching an instability displacement at mid-height. It was established that the experimentally observed behaviour of posttensioned masonry walls shows good agreement with the values predicted using Equations 1, 3 and 6.

The negatively sloped post-peak force-displacement behaviour of PTO-03 was most likely due to yielding of the mild steel threaded bar, with similar behaviour previously reported by Bean Popehn et al. (2007). The measured force-displacement hysteretic curves for PTO-05 to PTO-07 at small displacements show a mid-height displacement occurring with little or no lateral force measured, which was either due to the formation of a gap on both sides of the test walls (between the backing frame and the wall) or due to the absence of tendon restraint. In the latter case, the wall behaved similarly to an as-built wall until the strand touched the conduit walls and started to elongate, resulting in increased flexural capacity. It was therefore established that use of mechanical restraints inside a cored cavity is warranted, to restrain the PT tendon.

Tendon Stress

Flexural bending of the out-of-plane loaded posttensioned walls generates deformation between the tendon anchorages at the top and bottom of the walls, which causes elongation of the tendon and increases the tendon tensile stress. For all test walls the measured tendon stress was plotted against the lateral displacement at mid-height as shown in

Fig. 8, with the strand stress increasing linearly without exceeding specified elastic limits, except for PTO-03. For test wall PTO-03, the tendon stress reached its yield strength at 14 mm lateral displacement, and once the bar had possibly yielded the maximum tendon force was reduced during subsequent loading cycles. A ductile and nonlinear elastic behaviour was observed in walls PTO-04 to PTO-08, with strand stress not exceeding the specified elastic limit and the wall returning to its original position. For test walls PTO-04 to PTO-08, minor stress loss was observed following the conclusion of testing to large displacement excursions. It was also established from testing results that in order for posttensioned masonry walls to exhibit ductile behaviour, the restoring force provided by the PT tendon must be maintained and design must ensure that the increased tendon stress does not exceed the tendon yield strength.

Wall Secant Stiffness

Quantification of wall stiffness is important when performing a non-linear analysis of a posttensioned masonry wall and therefore the variation in wall secant stiffness was investigated. For each displacement excursion secant stiffness, K, was calculated using Equation 8, where F_+ and F_- are the maximum measured forces; and D_+ and D_- are the corresponding measured displacements.

$$K = \frac{F_+ - F_-}{D_+ - D_-} \tag{8}$$

The calculated wall secant stiffness values are plotted against the amplitude of corresponding displacement cycle in Fig. 9(a). The wall secant stiffness at or prior to first cracking varied for the test walls and was observed to be directly proportional to the magnitude of applied posttensioning. The wall secant stiffness was observed to gradually decrease upon the application of subsequent loading cycles and was dependent on the extent of damage. The results favoured the use of secant stiffness to maximum strength, rather than

initial stiffness, for use in non-linear analysis of posttensioned clay brick masonry walls, which was consistent with the findings of a precedent study involving non-linear time history analyses and shaking table testing (Griffith et al. 2003). A procedure for calculating the secant stiffness for a simplified non-linear analysis of rocking walls has been discussed in ASCE 41-06 (2006).

Hysteretic Energy Dissipation

Hysteretic energy dissipated in each cycle was calculated by integrating the area enclosed between the loading and unloading curve of each loading cycle and is plotted against the amplitude of the corresponding displacement cycle in Fig. 9(b). In general, posttensioned walls exhibited a bi-linear elastic behaviour and small energy dissipation prior to tendon yielding, except for test wall PTO-04. The larger energy dissipation observed in PTO-04 may be attributed to localised material deterioration and the anisotropic nature of heterogeneous masonry materials. It was established from the results that the posttensioning seismic retrofit increased the wall capacity to withstand higher energy demand and that energy dissipated in a displacement excursion was a function of the wall damage. In seismic design of structures energy dissipation characteristics are crucial and are typically quantified by toughness modulus, T. The toughness modulus corresponding to each test wall was calculated by dividing the cumulative hysteretic energy by the volume of the masonry wall (refer Table 4).

Damping Ratio

For each displacement cycle an equivalent viscous damping ratio was calculated from experimental results using the method detailed in Chopra (2007), which is presented by Equation 9, where ξ = equivalent viscous damping ratio; E_D = area between loading and unloading curve; and E_{SO} = area of right angle triangle, with the vertical side of the triangle

representing the maximum measured force and the horizontal side of the triangle representing the corresponding displacement.

$$\xi = \frac{E_D}{2\pi E_{SO}} \tag{9}$$

The calculated equivalent viscous damping ratios for each displacement cycle are plotted against the amplitude of the corresponding displacement cycle (refer Fig. 9(c)). It was established from Fig. 9(c) that damping was independent of the level of applied posttensioning, being consistent with the analytical formulation presented by Sorrentino et al. (2008). Moreover, the average hysteretic damping observed for the test walls was similar to the code recommended value of 15% (NZS 2004) and remained more than 5% throughout the testing program. Griffith et al. (2003) proposed a lower bound damping value of 5% for analysing the non-linear behaviour of out-of-plane loaded clay brick masonry walls that fits well with the observations of this experimental program.

Conclusions

Predictive equations were presented for a posttensioned seismic retrofit design and the adequacy of these predictive equations was confirmed later by comparing predicted response parameters with experimental results. A total of eight (08) full scale slender masonry walls were tested by applying pseudo-static out-of-plane cyclic loading. Of these, two (02) test walls were tested as-built and six (06) test walls were seismically retrofitted by applying different magnitudes of posttensioning prior to testing. Masonry material properties were determined using standardised test procedures. Uniformly distributed out-of-plane cyclic loading was applied by alternatively inflating and deflating multiple air bags (two in series 1 and four in series 2), emulating seismic forces generated due to wall self-weight. Numerous characteristics pertaining to the out-of-plane seismic behaviour of posttensioned masonry

walls were investigated and are reported. The key findings of the experimental program are:

1. A single horizontal crack at or near mid-height was observed in all tests except PTO-08, confirming that the boundary conditions used in response prediction are appropriate and that there was no rotational restraint at the top and bottom of the wall.

2. The out-of-plane loaded posttensioned masonry walls failed in a displacement critical rocking mode and exhibited a self-centering response, which is advantageous for enabling immediate occupancy after an earthquake.

3. A bi-linear elastic behaviour was observed for test walls that were posttensioned using a strand, whereas strength degradation attributed to tensile yielding of the bar was observed in the wall that was posttensioned using a threaded mild steel bar. It was established from the test results that a posttensioning retrofit design should ensure that the tendon stress will not exceed the tendon yield strength.

4. Structural performance of masonry walls was improved after posttensioning, with the flexural strength of posttensioned masonry walls ranging from 300% to 805% of that measured for an as-built tested wall.

5. Out-of-plane flexural capacity of the test walls was predicted using the proposed equations and was then compared to experimental results, with the results of this comparison showing reasonable agreement between the predicted and observed behaviour.

6. Initial stiffness of test walls varied depending upon the magnitude of initially applied posttensioning, with wall secant stiffness for all test walls decreasing upon the application of subsequent displacement cycles. Based on this observation it is suggested that for

predicting post-cracking behaviour of posttensioned masonry walls, the use of secant stiffness to maximum strength is more appropriate than initial stiffness.

Acknowledgments

Financial support was provided by the New Zealand Foundation for Research Science and Technology through grant UOAX0411. Reid Construction Systems (New Zealand) supplied posttensioning materials and provided assistance with testing. The Higher Education Commission of Pakistan provided funding for the doctoral studies of the first author.

References

Al-Manaseer, A. A., and Neis, V. V. (1987). "Load tests on post-tensioned masonry wall panels." *ACI Structural Journal*, 84(6), 467-472.

American Society of Civil Engineers (ASCE). (2006). *ASCE/SEI 41-06: Seismic rehabilitation of existing buildings*, Reston, USA.

American Society for Testing and Materials International (ASTM). (2002). *ASTM C109/C109M-02: Standard test method for compressive strength of hydraulic cement mortar*, West Conshohoken, USA.

American Society for Testing and Materials International (ASTM). (2003). *ASTM C270-03: Standard test method for compressive strength of masonry prisms*, West Conshohoken, USA.

American Society for Testing and Materials International (ASTM). (2004). *ASTM C62-04: Standard specification for building brick- solid masonry units made from clay or shale*, West Conshohoken, USA.

Bean Popehn, Jennifer R., Schultz, Arturo E. and Drake, Christopher R. (2007). “Behavior of slender, posttensioned masonry walls under transverse loading.” *ASCE Journal of Structural Engineering*, 133(11), 1541-1550.

Bean Popehn, J. R., and Schultz, A. E. (2010). "Design provisions for post-tensioned masonry walls loaded out-of-plane." *The Masonry Society Journal*, 28(2), 9-26.

British Standards Institution (BS). (1985). BS 5628:1985-2: British standard code of practice for use of masonry. Part 2: Structural use of reinforced and prestressed masonry, London, UK.

British Standards Institution (BS). (1995). *BS 5628:1995-2: British standard code of practice for use of masonry. Part 2: Structural use of reinforced and prestressed masonry*, London, UK.

British Standards Institution (BS). (2000). *BS 5628:2000-2: British standard code of practice for use of masonry. Part 2: Structural use of reinforced and prestressed masonry*, London, UK.

Chopra, A. K. (2007). *Dynamics of structures: Theory and applications to earthquake engineering*, Prentice Hall, Upper Saddle River, UK.

Canadian Standards Association (CSA). (2004). *CSA S304.1-04: Design of masonry structures*, Mississauga (Ontario), Canada.

Curtin, W. G., Shaw, G., Beck, J. K., and Parkinson, G. I. (1984). "Masonry fin walls." *Structural Engineer*, 62(7), 203-210.

Derakhshan, H. (2011). "Seismic assessment of out-of-plane loaded unreinforced masonry walls." *Ph.D. Thesis, Depart. of Civil and Environmental Eng., University of Auckland, Auckland, New Zealand.*

Dizhur, D., Ismail, N., Knox, C., Lumantarna, R., and Ingham, J. M. (2010). "Performance of unreinforced and retrofitted masonry buildings during the 2010 Darfield earthquake." *Bulletin of the New Zealand Society for Earthquake Engineering*, 43(4), 321-339.

European Committee for Standardization (CEN). (1995). *EN 1996-1-1:1995 - Eurocode 6: Design of masonry structures - Part 1-1: General rules for reinforced and unreinforced masonry structures*, Brussels, Belgium.

European Committee for Standardization (CEN). (2005). *EN 1996-1-1:2005 - Eurocode 6: Design of masonry structures - Part 1-1: General rules for reinforced and unreinforced masonry structures*, Brussels, Belgium.

European Committee for Standardization (CEN). (2005). *Eurocode 8: Design of structures for earthquake resistance - Part 3: Assessment and retrofitting of buildings*, Brussels, Belgium.

Ewing, B. D., and Kowalsky, M. J. (2004). "Compressive behavior of unconfined and confined clay brick masonry." *Journal of Structural Engineering*, 130(4), 650-661.

Federal Emergency Management Agency (FEMA). (2006). *FEMA 547-06: Techniques for the seismic rehabilitation of existing buildings*, Washington, DC, USA.

Ganz, H. R. (1996). "VSL's experience with post-tensioned masonry." 1996 CCMS of the ASCE Symposium in Conjunction with Structures Congress XIV, ASCE, Chicago, IL, USA, 25-36.

Griffith, M. C., Magene, G., Melis, G., and Picchi, L. (2003). "Evaluation of out-of-plane stability of unreinforced masonry walls subjected to seismic excitation." Journal of Earthquake Engineering, 7(1), 141-169.

Ingham, J. M., and Griffith, M. (2011). "Performance of unreinforced masonry buildings during the 2010 Darfield (Christchurch, NZ) earthquake." Australian Journal of Structural Engineering, 11(3), 207-224.

Ingham, J. M., Biggs, D. T., and Moon, L. M. (2011). "How did unreinforced masonry buildings perform in the February 2011 Christchurch earthquake?" The Structural Engineer, 89(6), 14-18.

Ismail, N., Lazzarini, D. L., Laursen, P. T., and Ingham, J. M. (2011). "Seismic performance of face loaded unreinforced masonry walls retrofitted using posttensioning." Australian Journal of Structural Engineering, 11(3), 243-252.

Ismail, N. (2011). "Unbonded post-tensioning", Assessment and improvement of unreinforced masonry buildings for earthquake resistance, J. M. Ingham, ed., New Zealand Society for Earthquake Engineering, Wellington, New Zealand.

Krause, G. L., Devalapura, R., and Tadros, M. K. (1996). "Testing of prestressed clay brick walls." 1996 CCMS of the ASCE Symposium in Conjunction with Structures Congress XIV, Chicago, IL, USA.

Laursen, P. T. (2002). "Seismic analysis and design of post-tensioned concrete masonry walls." Ph.D. Thesis, Depart. of Civil and Environmental Eng., University of Auckland, Auckland, New Zealand.

New Zealand Society for Earthquake Engineering (NZSEE). (2006). *Assessment and improvement of the structural performance of buildings in earthquakes: Recommendations of a NZSEE study group on earthquake risk buildings*, Wellington, New Zealand.

New Zealand Transportation Agency (NZTA). (2010). "Moving the Rob Roy." New Zealand Herald, Auckland. <http://www.nzherald.co.nz/nz/news/video.cfm?c_id=1&gal_objectid=10670092&gallery_id=113594> (July 23, 2011).

Scolforo, M. J. (1996). "Proposed prestressed masonry design provisions." *Proc., 1996 CCMS of the ASCE Symposium in Conjunction with Structures Congress XIV*, Chicago, USA, 15-18 April.

Schultz, A. E., and Scolforo, M. J. (1991). "An overview of prestressed masonry." *The Masonry Society Journal*, 10(1), 6-21.

Sorrentino, L., Masiani, R., Griffith, M.C. (2008). "The vertical spanning strip wall as a coupled rocking rigid body assembly." Structural Engineering and Mechanics, 29(4), 433-453.

Standards Australia International (AS). (1998). *AS 3700-98: Masonry structures*, Sydney, Australia.

Standards Australia International (AS). (2001). *AS 3700-01: Masonry structures*, Sydney, Australia.

Standards Australia International (AS). (2003). *AS/NZS 4456.15: Masonry units and segmental pavers and flags-methods of test-determining lateral modulus of rupture*, Sydney, Australia.

Standards New Zealand (NZS). (1990). *NZS 4230-90: Code of practice for the design of concrete masonry structures*, Wellington, New Zealand.

Standards New Zealand (NZS). (2004). *NZS 4230-04: Design of reinforced concrete masonry structures*, Wellington, New Zealand.

The Masonry Society (MSJC). (1995). *ACI 530-95/ASCE 5-95/TMS 402-95: Building code requirements for masonry structures*, Boulder, CO, USA.

The Masonry Society (MSJC). (2002). *ACI 530-02/ASCE 5-02/TMS 402-02: Building code requirements for masonry structures*, Boulder, CO, USA.

The Masonry Society (MSJC). (2005). *ACI 530-05/ASCE 5-05/TMS 402-05: Building code requirements for masonry structures*, Boulder, CO, USA.

The Masonry Society (MSJC). (2008). *ACI 530-08/ASCE 5-08/TMS 402-08: Building code requirements for masonry structures*, Boulder, CO, USA.

Wight, G. D. (2006). "Seismic performance of a post-tensioned concrete masonry wall system " Ph.D. Thesis, Depart. of Civil and Environmental Eng., University of Auckland, New Zealand.

List of Figures

1 Tables

2 **Table 1.** Masonry stress block parameters at nominal strength

Reference	Brick Masonry	
	α	**β**
BS 5628 (BS 2000)	0.50	1.00
TMS 402 (MSJC 2005)	0.50	1.00
TMS 402 (MSJC 2008)	0.80	0.80
AS 3700 (AS 2001)	1.10	0.85
S 304.1 (CSA 2004)	0.85	-
EC 8 (CEN 2005)	0.86*	-
NZS 4230 (NZS 2004)	0.85	0.85
Ewing and Kowalsky (2004)	0.93	0.66

Where: α = depth of equivalent stress block; and β = width of equivalent stress block.

*Calculated from inverse function as (i.e., 1/1.15 = 0.86)

1 **Table 2.** Test wall details

Test Series	Test Wall	Tendon Type	h_e (mm)	l_w (mm)	b_w (mm)	W_w (kN)	P_i (kN)	f_{psi} (MPa)	f_{psi}/f_{py} (ratio)	f_{mb} [a] (MPa)	f'_m (MPa)	f_{mb}/f'_m (ratio)
1	ABO-01	-	4100	1170	220	19.0	-	-	-	-	10.7	-
2	ABO-02	-	3670	1170	220	17.9	-	-	-	-	8.7	-
1	PTO-03	B[b]	4100	1170	220	19.0	50	442	0.88	0.27	10.7	0.03
1	PTO-04	S[c]	4100	1170	220	19.0	100	1013	0.60	0.46	10.7	0.04
2	PTO-05	S[c]	3670	1170	220	17.9	50	506	0.30	0.26	8.7	0.03
2	PTO-06	S[c]	3670	1170	220	17.9	70	709	0.42	0.34	8.7	0.04
2	PTO-07	S[c]	3670	1170	220	17.9	100	1013	0.60	0.46	8.7	0.05
2	PTO-08	S[c]	4100	1170	220	19.5	100	1013	0.60	0.46	8.7	0.05

Where: h_e = wall height; l_w = wall length; b_w = wall thickness; W_w = wall self-weight; P_i = applied initial posttensioning force; f_{psi} = applied initial tendon stress; f_{py} = tendon yield stress; f_{mb} = compression stress at the base of the wall; and f'_m = masonry compressive strength.

[a] $f_m = (N_t + W_w + f_{se}A_{ps})/l_w b_w$

[b] 12 mm threaded steel bar (A_{ps} = 113.1 mm^2; f_{py} = 500 MPa; f_{pu} = 680 MPa; E_{ps} = 200 GPa)

[c] 12.7 mm sheathed, greased seven-wire strand (A_{ps} = 98.7 mm^2; f_{py} = 1680 MPa; f_{pu} = 1860 MPa; E_{ps} = 200 GPa)

Table 3. Masonry material properties

Property Units	Test Series	f'_b MPa	f'_j MPa	f'_m MPa	f_r MPa	C MPa	μ
Value	1	39.4	1.4	10.7	0.09	0.1	0.47
COV		28%	8%	33%	29%	-	-
Value	2	21.4	1.4	8.7	0.08	0.1	0.67
COV		23%	8%	30%	66%	-	-

Where: f'_b = brick compressive strength; f'_j = mortar compressive strength; f'_m = masonry compressive strength; f_r = tensile strength of masonry; C = masonry cohesion; and μ = masonry coefficient of internal friction.

Table 4. Test Results

Test Wall	M'_c kN.m	V'_c kN	f_{ps} MPa	M_n kN.m	V_n kN	M_c kN.m	V_c kN	M_u kN.m	V_u kN	V_c/V'_c ratio	V_u/V_n ratio	γ_u %	T kPa	V_u/V_o %
ABO-01	1.3	2.5	-	-	-	2.3	4.4	-	-	1.76	-	5.1	-	100
ABO-02	1.1	2.3	-	-	-	1.7	3.8	-	-	1.63	-	3.0	0.27	100
PTO-03	3.0	5.9	476	6.8	13.2	6.5	12.7	6.8	13.2	2.15	1.00	4.7	1.31	300
PTO-04	4.9	9.5	1149	12.8	25.0	11.0	21.5	15.0	29.2	2.26	1.17	4.8	3.4	664
PTO-05	2.9	6.3	656	7.7	16.9	3.8	8.3	9.3	20.2	1.31	1.20	4.2	0.71	532
PTO-06	3.6	7.9	859	9.8	21.3	5.4	11.7	11.8	25.8	1.48	1.21	4.2	1.36	679
PTO-07	4.7	10.3	1163	12.7	27.6	9.7	21.1	14.0	30.6	2.04	1.11	4.1	1.89	805
PTO-08	4.3	9.3	1147	11.3	24.6	8.2	17.8	10.5	22.9	1.91	0.93	0.9	0.24	603

Where: M'_c = predicted nominal flexural strength; V'_c = predicted lateral force at first cracking; f_{ps} = predicted tendon stress at nominal strength; M_n = predicted nominal flexural strength; V_n = predicted lateral force at nominal strength; M_c = measured analogous moment at first cracking; V_c = measured lateral force at first cracking; M_u= maximum measured analogous moment; V_u= measured maximum lateral force; V_o= measured maximum lateral force for as-built tested wall; γ_u= measured maximum drift ratio; and T = wall toughness modulus.

(a) coring operation for internal posttensioning (b) external posttensioning

1 **Figure 1.** Posttensioning seismic retrofitting

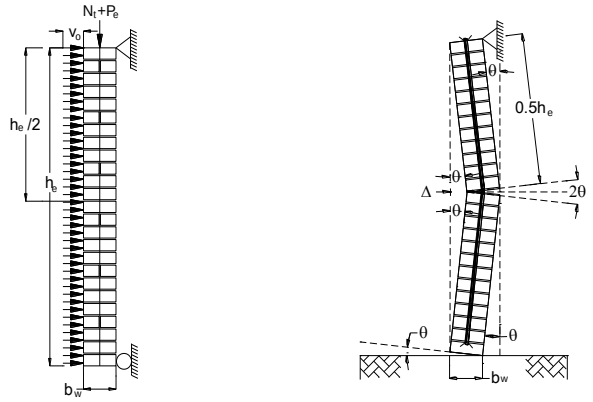

(a) applied forces (b) wall deformation

Figure 2. Wall definitions

1

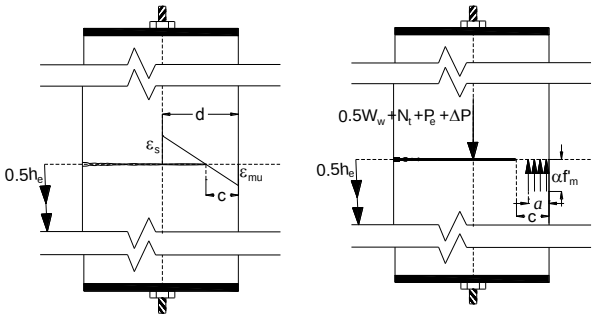

(a) strain profile (b) stress profile

Figure 3. Mid-height hinge location at nominal strength

1

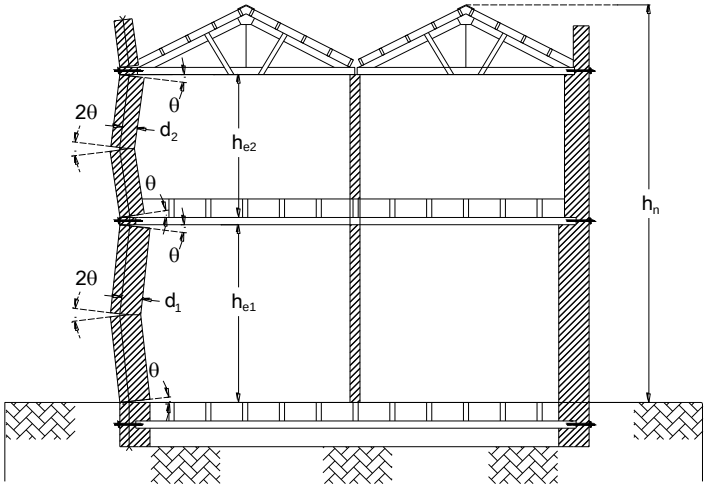

Figure 4. Deflected multi-storey posttensioned masonry wall

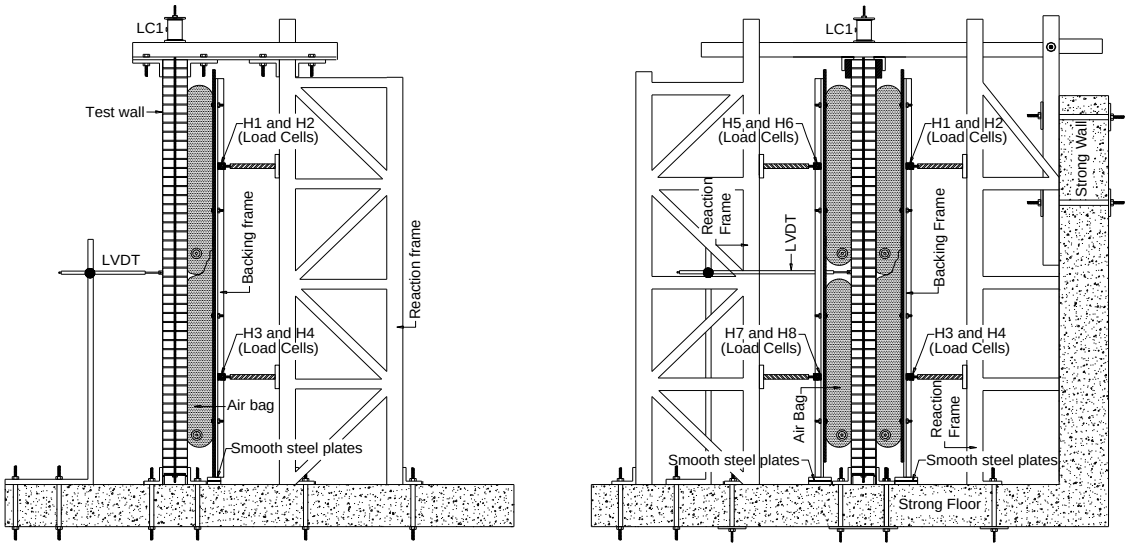

(a) series 1 (b) series 2

Figure 5. Test setup details

(a) setup for testing

(b) series 1 testing

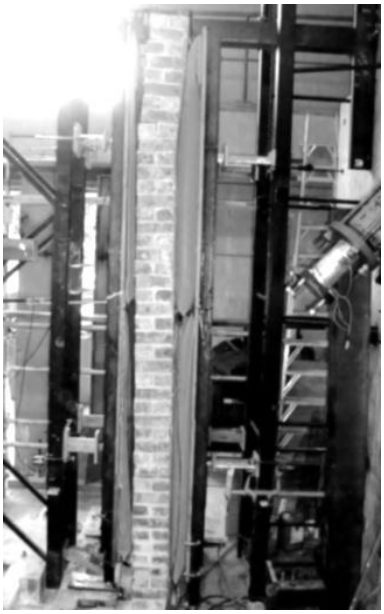

(c) series 2 testing

Figure 6. Photographs of testing

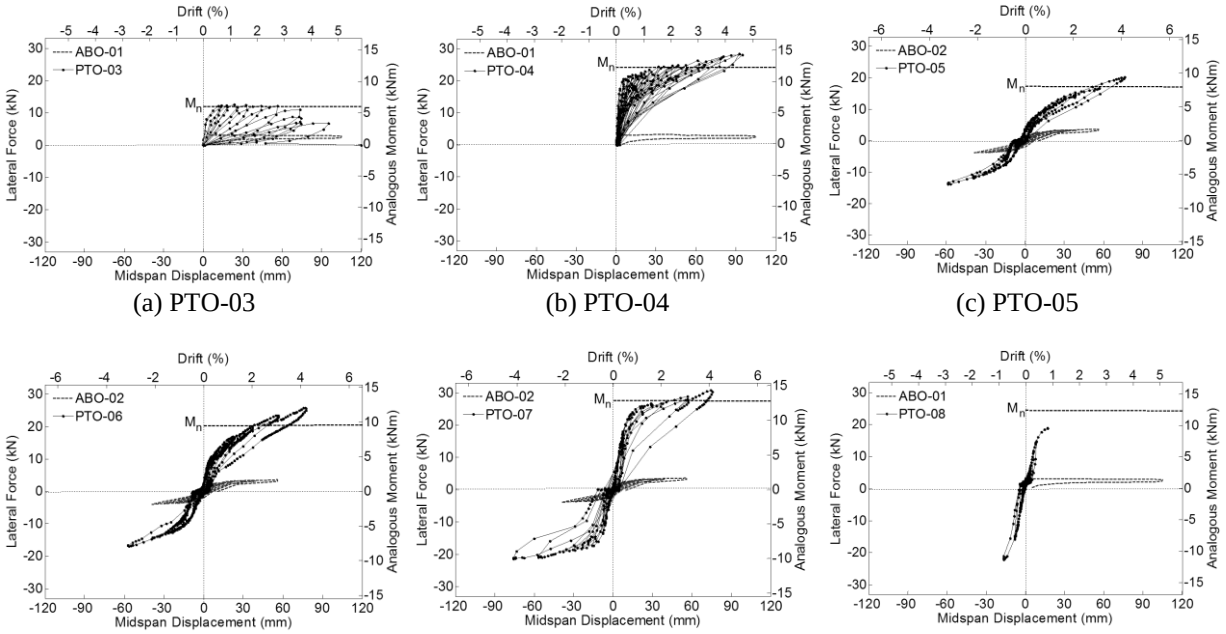

Figure 7. Force-displacement curves

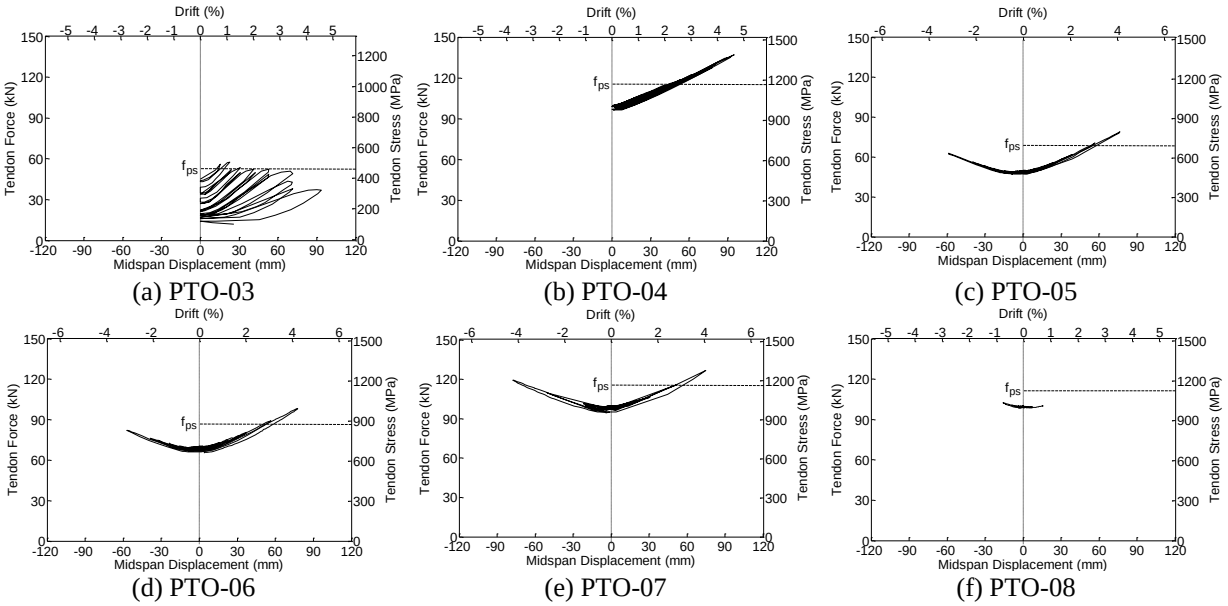

Figure 8. Tendon force-displacement curves

1

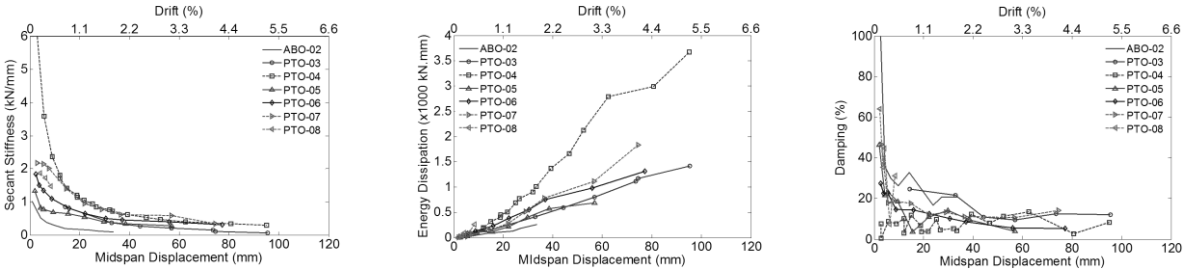

(a) secant stiffness (b) cumulated dissipated energy (c) damping ratio

Figure 9. Seismic response parameters

1